A COMPREHENSIVE FOOT MODEL FOR GAIT ANALYSIS OF PATIENTS WITH PSORIATIC ARTHRITIS

Miguel Nobre Castro
Master of Science Degree in Biomedical Engineering
Instituto Superior Técnico, Universidade de Lisboa
December 2013

Abstract: The psoriatic arthritis (PsA) is a disease that evolves from skin psoriasis affecting 25% of these patients. This chronic disease is characterized by the appearance of localized joint inflammation and pain which is triggered by mechanical loads acting on the bones, tendons and ligaments leading to bone deformation and conditioning patients' mobility. To assess the level of feet impairment that changes the gait patterns in these patients, a biomechanical foot model with 4+2 (shank and single foot) segments is used in this study being simultaneously applied to both feet, with a 25 marker protocol per limb. The objective of this study is to analyse the gait parameters such as the inter-segment kinematics, kinetics, plantar pressures distribution and spatiotemporal at specific events of stance phase in two different groups: a 10 (5M/5F) healthy individuals group and another of 8 (5M/3F) patients with PsA. To highlight deviations in pathological gait at the early stage of the disease (patients with less than 2 years of disease duration) a statistical comparison is performed using the Welch's t-test and Mann-Whitney U tests among the gait parameters. Since the statistically significant results are few even using these two tests, the analysis of the statistical trends is also done. The results of these approaches confirm most of the deformities in the patients such as small ranges of motion in ankle and foot's joints, pes planovalgus (flat foot) and claw toe, which all converge to adapted gait patterns.

Keywords: Psoriatic arthritis; Multisegment foot model; Kinematics; Kinetics; Kinematic consistency; Euler angles.

1. Introduction

Psoriatic arthritis (PsA) is defined as an inflammatory arthropathy characterized by stiffness, pain, swelling and tenderness of the joints as well as of the surrounding ligaments and tendons, which can evolve from a non-destructive arthritis into an erosive one conditioning patient's quality of life. About 25% of the individuals that present clinical history of skin psoriasis in the past years develop PsA (Gottlieb *et al*., 2008). This disease spreads through limbs' extremities mainly affecting feet bones which deform as the disease progresses leading to localized inflammation and pain in joints and consequent loss of mobility. Therefore, patients with PsA will manifest adapted gait patterns due to altered foot function (Hyslop *et al*., 2010).

This study focuses attention on the early stage of the disease trying to trace at least some differences in gait patterns and non-coherent biomechanical parameters between the control individuals and PsA patients during the stance phase of a gait cycle.

A multi-segment foot model may, thus, provide a more complete description of gait abnormalities where pathology is present at multiple joints as the case of PsA and varied patterns of impairment can be obtained (Woodburn *et al*., 2004). There are many multi-segment foot models in the literature and some of them cover more than three foot segments (Hyslop *et al*., 2010; Jenkyn *et al*., 2009; Leardini *et al*., 1999; MacWilliams *et al*., 2003; Nester *et al*., 2007; Tome *et al*., 2006).

2. Experimental Protocol

2.1. Data Acquisition Instrumentation

The biomechanical assessment of patients' feet function can help to understand how this disease is triggered. It is important to determine the gait parameters for all individuals, such as the spatiotemporal, plantar pressure distribution, inter-segment kinematics and forces in play.

The assessment is started by asking the subject to walk barefoot over a pressure sensing walkway (GAITRite, CIR Systems, Clifton, NJ, USA). This carpet-

like instrument spatially identifies subject's footprints along its extension and with this information time-distance parameters are calculated. Its internal software computes among others the walking velocity, stride length, stance and swing phases' duration.

The Footscan device which is also a pressure plate instrument (Footscan®, RS Scan International, Olen, Belgium) measure gait parameters such as plantar contact areas and peak pressures measured at each sensor.

The inter-segment kinematics is the measurement of the relative movements of rotation between adjacent rigid bodies that constitute the biomechanical model. Subjects are instrumented with reflective markers placed on the skin right above specific bone landmarks (reached through palpation), which define the model and an acquisition is made using a Qualsys® motion capture system and QTM software (Qualisys ProReflex System, Qualisys, Gothenburg, Sweden). The force platforms (Advanced Mechanical Technologies, Inc., Watertown, MA, USA) work with appropriate transducers and synchronized with the motion capture system enabling to quantify the ground reaction forces.

All these equipment are available at the Lisbon Biomechanics Laboratory (LBL, at IST).

2.2. Biomechanical Foot Model

The original foot model purposed by Hyslop *et al*. (2010) in the study of the Scottish population with PsA has five segments. The current work adopts only four of those segments. Therefore, the original foot model divides the leg and foot by the following five segments: the Rearfoot, which considers the region between the ankle joint and transverse tarsal joint including the talus and calcaneus bones; the Midfoot, dedicated on the distal row of the five tarsal bones; the First Metatarsal, which refers simply to the first metatarsal bone; the Lateral Forefoot that joins the other four metatarsal bones, from II to V; the Hallux, as the great digit/toe. In addiction the extra segments are: the Shank that covers the whole leg and serves as the anatomical reference for rearfoot motion and the Single Foot segment which evaluates the global foot function.

Apart from the first metatarsal which is a single bone, all other segments in the model are composed by two or more bones.

Movements of joint rotation mainly occur in anatomical planes around imaginary axes. If a perpendicular axis is defined in respect to an anatomical plane of a given rigid body (segment), a rotation that happens in that plane can be easily quantified as an angular range.

To define all these anatomical segments, a multibody system arranged in an open-loop kinematic chain structure is considered, in which a system of axes (the reference frame) is defined per each one of the rigid bodies in order to relate its position and orientation with respect to its predecessors in the global reference frame of the laboratory. This is possible through a 25 markers protocol one foot and shank (a sum of 50), which are strategically positioned on skin as suggested by Figure 1 and Figure 2.

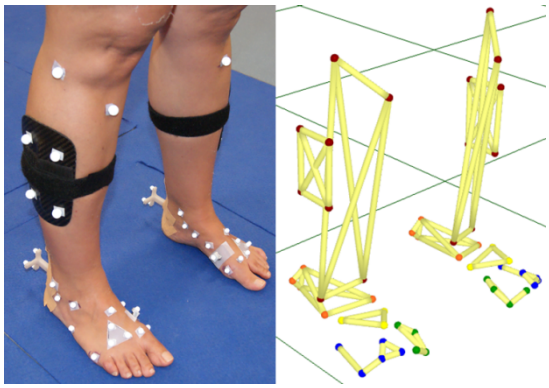

Figure 1: Photography of the 25 markers protocol applied on each individual's lower limb (left). The three-dimensional reconstruction of the reflective markers in the laboratory space by the Qualisys® Track Manager (QTM) software (right).

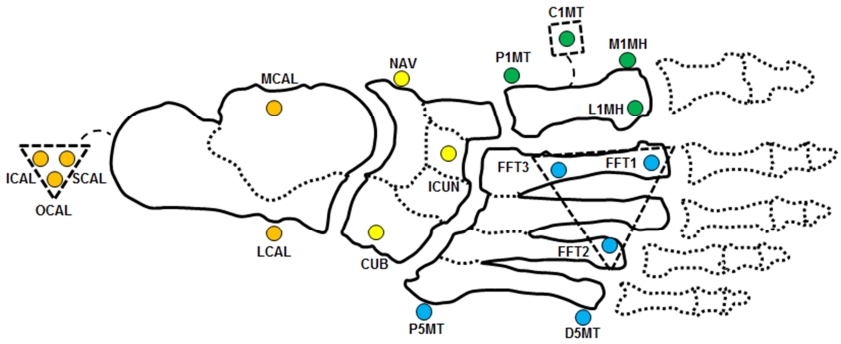

Figure 2: Representation of the 4+2 segments biomechanical foot model used in the study with focus on the foot bones' landmarks.

Hyslop *et al*. (2010) defined that the reference frame of a rigid body lies in the most proximal point of it, being coherent with its proximal joint region. Therefore, since the z-axis generally points upwards and y-axis generally points forwards, the respective x-axis must always point to right side of the body regardless of the side of the body where rigid body belongs (see Figure 3). This guarantees a direct reference frame.

Despite the fact that the selected markers were chosen taking into account the procedure reported in Hyslop *et al*. (2010), the reference frame of each rigid body is not exactly reconstructed in the same way. As a matter of fact, some readjustments are made in order to give priority to some of the three axes always keeping in mind that they must work as a direct reference frame. Positive rotations around axes always agree with the right-hand rule.

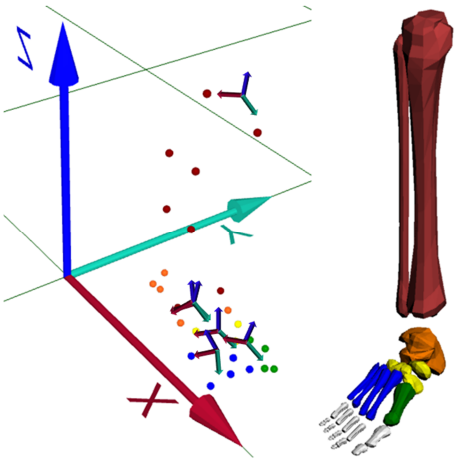

Figure 3: Three-dimensional representation of all local reference frames of the rigid bodies in the global reference frame of the laboratory. The x-axis of the global reference frame corresponds to the walking direction. The x-axis of each local reference frame points to the right i.e. it almost coherent with the negative global y-axis.

Therefore, the shank is described by 8 brown makers (HFIB, TTUB, MMAL, LMAL, SHN1-4) (not represented in Figure 2), last three of which are part of a cluster (see Figure 1) and are just tracking markers. Its rotations around its axes does not correspond to any anatomical movements since there is a lack of a thigh segment, hence, it is described in the global reference frame.

The rearfoot is described through 5 orange markers (SCAL, ICAL, OCAL LCAL MCAL), first three of which are part of skin-mounted wand and both anatomical and tracking markers. The rotations about x-axis, y-axis and z-axis correspond to: dorsiflexion(+)/plantarflexion(-), inversion(+)/eversion(-) and internal(+)/external(-) rotations, respectively.

The midfoot is described by 3 yellow markers (NAV, ICUN, CUB) which are both anatomical and tracking markers. The rotations about x-axis, y-axis and z-axis correspond to: dorsiflexion(+)/plantarflexion(-), inversion(+)/eversion(-) and adduction(+)/abduction(-), respectively.

The 1st metatarsal id described by 4 green markers (P1MT, M1MH, L1MH and C1MT), being L1MH just anatomical and C1MT (in a skin-mounted wand) just tracking markers, while the other two are both. The rotations about x-axis, y-axis and z-axis correspond to: dorsiflexion(+)/plantarflexion(-), inversion(+)/eversion(-) and abduction(+)/adduction(-), respectively.

The lateral forefoot is described through 5 blue markers (P5MT, D5MT, FFT1-3), which FFT1-3 markers cosrrespond to a skin-mounted plate/cluster are the tracking markers. The rotations about x-axis, y-axis and z-axis correspond to: dorsiflexion(+)/plantarflexion(-), inversion(+)/eversion(-) and adduction(+)/abduction(-), respectively.

Last but not least, the single foot is a different segment since it is described through markers from all the other foot's rigid bodies (SCAL, ICUN, M1MH, FFT2). The rotations about x-axis, y-axis and z-axis correspond to: dorsiflexion(+)/plantarflexion(-), inversion(+)/eversion(-) and internal(+)/external(-) rotations, respectively.

3. Computational Methods

3.1. Raw Data Filtering

The markers' trajectories are extracted from the laboratory during the acquisition through the Qualisys® motion capture system and due to the use of these optoelectronic devices the electronic noise is inherently present The noise spreads along the high frequencies of a signal and it can be seen through a spectral analysis of a non-filtered signal. Then the digital filtering must be done resourcing to a low-pass filter centred on that f_c which permits the attenuation of the higher frequencies if one choses a low f_c the noise is much more attenuated indeed, but simultaneously some signal distortion takes place; on the other hand, an high f_c results on lower signal distortion along with much more coupled noise (Winter, 1990)

This current work follows the estimation of the cut-off frequency achievement through a residual analysis approach stated by Winter (1990). From the 0.5 Hz to 20 Hz of possible frequencies, a second order low-pass filter is used to obtain the filtered data. The interval of frames from the raw data where the analysis will be performed must contain 10 frames in the beginning plus 10 frames at the end for the filter to be applied twice (because the first time it is applied a delay is induced on

the data). This filter is already a MATLAB® algorithm called *filtfilt()*. Therefore, the range of possible frequencies from 7 Hz to 20 Hz is used to estimate the noise residual value at 0 Hz through a linear regression. The respective true value of f_c is then searched throughout an interpolated function covering these frequency values

3.2. Static Calibration

The static calibration procedure consists on the first complete reconstruction of the whole model through the anatomical markers and prior assembly of each body respect reference frames.

Since each rigid body is characterized by a local reference frame, a transformation matrix ${}^{0}_{A}\mathbf{T}$ can be assumed throughout the analysis such as

$${}^{0}_{A}\mathbf{T} = \begin{bmatrix} t_{11} & t_{12} & t_{13} & t_{14} \\ t_{21} & t_{22} & t_{23} & t_{24} \\ t_{31} & t_{32} & t_{33} & t_{34} \\ t_{41} & t_{42} & t_{43} & t_{44} \end{bmatrix} = \begin{bmatrix} {}^{0}_{A}\mathbf{R} & {}^{0}\mathbf{P}_{Aorg} \\ 0 & 1 \end{bmatrix}$$

A transformation matrix transforms points from the local reference frame 'A' to the coordinate system of the global reference frame '0' (laboratory's origin). This type of transformation matrix is the so-called homogenous transformation because it concatenates a rotation matrix ${}^{0}_{A}\mathbf{R}$ (3x3 matrix) along with a translation operation ${}^{0}\mathbf{P}_{Aorg}$ (3x1 vector/point), which corresponds to the coordinates of the origin point of the rigid body A.

This can be understood by the following Equation (1) reproduces the example of the Figure 4 which are in agreement with the principles stated by van den Bogert *et al*. (1994) to determine anatomical axes,

$${}^{0}\mathbf{P} = {}^{0}_{A}\mathbf{R}\,{}^{A}\mathbf{P} + {}^{0}\mathbf{P}_{Aorg} \qquad (1)$$

which is equivalent to the homogeneous transformation in Equation (2),

$${}^{0}\mathbf{P} = {}^{0}_{A}\mathbf{T}\,{}^{A}\mathbf{P} \qquad (2)$$

where ${}^{0}\mathbf{P}$ and ${}^{A}\mathbf{P}$ assume now the form ${}^{0}\mathbf{P} = \left\{ {}^{0}\mathrm{P}_x \;\; {}^{0}\mathrm{P}_y \;\; {}^{0}\mathrm{P}_z \;\; 1 \right\}^{\mathrm{T}}$ and ${}^{A}\mathbf{P} = \left\{ {}^{A}\mathrm{P}_x \;\; {}^{A}\mathrm{P}_y \;\; {}^{A}\mathrm{P}_z \;\; 1 \right\}^{\mathrm{T}}$.

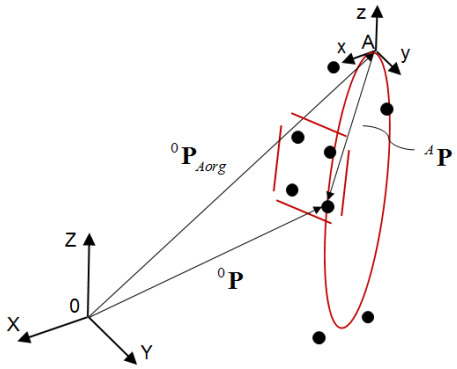

Figure 4: Representation of the local reference frame of rigid body 'A' described in the global reference frame of the laboratory '0'.

3.2.1. Optimization Step of Static Calibration

By definition, it is stated that the points that constitute a given rigid body must be kept equally spaced among themselves all over the analysis. So each rigid body local reference frames can be estimated directly through the anatomical markers or indirectly by resource of the tracking markers (throughout the walking analysis), with these latter allowing removal of the anatomical ones.

During the static acquisition period the individual mimics the anatomical reference position, forward facing the walking direction and keeping still. A total of N=100 frames from that acquisition data are.

Analysing each rigid body individually throughout that time interval, at each k acquisition's frame (time step) its transformation matrix ${}^{0}_{A}\mathbf{T}^{k}$ containing the local reference frame's axes is directly computed from the anatomical markers and another ${}^{0}\mathbf{X}^{k}$ matrix – the *global matrix of the tracking markers* – which columns constitute the rigid body's ${}^{0}\mathbf{P}_{m}$ M tracking markers in global coordinates is directly calculated, i.e.

$${}^{0}\mathbf{X}^{k} = \begin{bmatrix} {}^{0}\mathrm{P}_{1\,x} & \cdots & {}^{0}\mathrm{P}_{M\,x} \\ {}^{0}\mathrm{P}_{1\,y} & \cdots & {}^{0}\mathrm{P}_{M\,y} \\ {}^{0}\mathrm{P}_{1\,z} & \cdots & {}^{0}\mathrm{P}_{M\,z} \\ 1 & \cdots & 1 \end{bmatrix}.$$

The purpose of this optimization step described by this *cost function* $f({}^{A}\mathbf{X})$ in Equation (3) is to find the best *local matrix of the tracking markers*

$${}^{A}\mathbf{X}^{*} = \begin{bmatrix} {}^{A}x^{*}_{11} & \cdots & {}^{A}x^{*}_{1M} \\ {}^{A}x^{*}_{21} & \cdots & {}^{A}x^{*}_{2M} \\ {}^{A}x^{*}_{31} & \cdots & {}^{A}x^{*}_{3M} \\ {}^{A}x^{*}_{41} & \cdots & {}^{A}x^{*}_{4M} \end{bmatrix} = \begin{bmatrix} {}^{A}\mathrm{P}^{*}_{1\,x} & \cdots & {}^{A}\mathrm{P}^{*}_{M\,x} \\ {}^{A}\mathrm{P}^{*}_{1\,y} & \cdots & {}^{A}\mathrm{P}^{*}_{M\,y} \\ {}^{A}\mathrm{P}^{*}_{1\,z} & \cdots & {}^{A}\mathrm{P}^{*}_{M\,z} \\ {}^{A}x^{*}_{41} & \cdots & {}^{A}x^{*}_{4M} \end{bmatrix}$$ which

best describes the coordinates of the tracking markers

in the local reference frame all over those *N*=100 frames, substituting all the other matrices (${}^{0}\mathbf{X}^{k}$ and ${}^{0}_{A}\mathbf{T}^{k}$) calculated in a least squares approach. Since the homogenous transformation proprieties require that the bottom row of the ${}^{A}\mathbf{X}^{*}$ matrix must be composed by ones, *M* constraints must be fulfilled in the optimization process in Equation (4).

The localization of the rigid body on the global reference frame during the dynamic analysis is made through the tracking markers since their location on the local reference frame is known at each time step. Thus, this local matrix is invariant.

$$f({}^{A}\mathbf{X}) = \sum_{k=1}^{N} \| \, {}^{0}\mathbf{X}^{k} - {}^{0}_{A}\mathbf{T}^{k} \, {}^{A}\mathbf{X} \, \|^{2} \tag{3}$$

$$\min_{{}^{A}\mathbf{X}\in\mathbb{R}^{4,M}} f({}^{A}\mathbf{X}) = \sum_{k=1}^{N} \left(\sum_{i=1}^{4}\sum_{j=1}^{M}\sum_{l=1}^{4} ({}^{0}x_{ij}^{k} - t_{il}^{k} \, {}^{A}x_{lj}^{*})^{2} \right)$$

$$s.t. \tag{4}$$

$${}^{A}x_{4j}^{*} - 1 = 0 \quad j \in [1, M]$$

3.3. Inter-segment Kinematics Evaluation

3.3.1. Optimization Step of the Kinematic Consistency

During a dynamic trial, when a given rigid body needs to be tracked, in order to retrieve again its transformation matrix another issue is raised: both local and global matrices of these tracking markers are known, but even after the data filtering the global coordinates (${}^{0}\mathbf{X}$) of the tracking markers will certainly not be coherent with the ones that are saved on the ${}^{A}\mathbf{X}$ matrix from frame to frame. The distances between the markers are not equal to the ones called as invariant. This is known as the *Kinematic Consistency* problem.

The reflective markers are placed on skin and it moves away from the desired bone landmarks. They would be more distant form each other near articular joints where the skin is more elastic and stretches easily leading to displacement of the markers (Alonso et al., 2007; Silva & Ambrósio, 2002).

The *cost function* $f({}^{0}_{A}\mathbf{T})$ described in Equation (5) and is suggested which will focus on the search for the best transformation matrix ${}^{0}_{A}\mathbf{T}^{*}$ that fits the non-consistent data obtained from the digitalization process of the motion capture system.

The equality constraints that affect this cost function are not only focused on the proprieties of the bottom row of the homogenous transformation matrix but also concerning the proprieties the rotation matrix within the transformation matrix. Regarding to the transformation matrix, the first 4 equality constraints of the cost function in the optimization Equation (6) imposes three null entries and an entry with a one in the bottom row of the matrix. In respect to the rotation matrix, the three axes of the reference frame must always be orthogonal among them to constitute a direct reference frame. The same is valid for rows of the rotation matrix regarding its correspondent inverse/transpose matrix. Therefore, performing an external product between two column vectors of the rotation matrix should give rise to the third column vector and between two row vectors it should give rise to the third one. Since each cross product contributes with two equality constraint equations these correspond to 6 more equations.

Nevertheless, an orthonormal reference frame should fulfil also the condition of unitary vector for each column and row. Thus, another cross product should be added for the columns and another should be added for the rows. A third cross product for the columns and for the rows would be redundant. All together these equations correspond to 16 equality constraints for the cost function and simultaneously 16 design variables (the entries of a 4x4 transformation matrix), so the optimum transformation matrix can be implemented through an adapted Newton-Raphson method to speed up the computation time and effort. Joint constraints are not taken into account.

$$f({}^{0}_{A}\mathbf{T}) = \sum_{k=1}^{N} \| \, {}^{0}\mathbf{X}^{k} - {}^{0}_{A}\mathbf{T} \, {}^{A}\mathbf{X} \, \|^{2} \tag{5}$$

$$\min_{\mathbf{T}\in\mathbb{R}^{4,4}} f({}^{0}_{A}\mathbf{T}) = \sum_{i=1}^{4}\sum_{j=1}^{M}\sum_{l=1}^{4} ({}^{0}x_{ij} - t_{il}^{*} \, {}^{A}x_{lj})^{2}$$

$$s.t.,$$

$$t_{4l}^{*} = 0 \quad l \in [1,3];$$

$$t_{44}^{*} - 1 = 0; \tag{6}$$

$$\mathbf{t}_{i1}^{*} \times \mathbf{t}_{i2}^{*} - \mathbf{t}_{i3}^{*} = 0 \quad i \in [1,3];$$

$$\mathbf{t}_{i2}^{*} \times \mathbf{t}_{i3}^{*} - \mathbf{t}_{i1}^{*} = 0 \quad i \in [1,3];$$

$$\mathbf{t}_{1l}^{*} \times \mathbf{t}_{2l}^{*} - \mathbf{t}_{3l}^{*} = 0 \quad l \in [1,3];$$

$$\mathbf{t}_{2l}^{*} \times \mathbf{t}_{3l}^{*} - \mathbf{t}_{1l}^{*} = 0 \quad l \in [1,3].$$

Note that a similar but limited approach is stated by Ojeda *et al*. (2011) called as the Segmental Optimization method where the concerning of the constraint equations is that the vectors of the rotation matrix should be unitary but let inequality constraints such as the entries of the rotation matrix vary between the interval [-1,1] but do not guarantee the orthogonally between these vectors.

3.3.2. Static Analysis

To calculate the inter-segment kinematics it is important to define a baseline for these angles to be measured. This means that an anatomical reference position must be defined (as it was already stated), in order to obtain those measured angles that correspond to zeros (the so-called off-set angles) and all the rotation movements that happens from these angles have already the meaning of some movement throughout an anatomical plane.

considering now two rigid bodies, A and B, represented in the Figure 5 where the rigid body A is the parent of B, the three measured off-set angles calculated for the anatomical reference position are then be subtracted to the measurements made later during each time step of the dynamic trials.

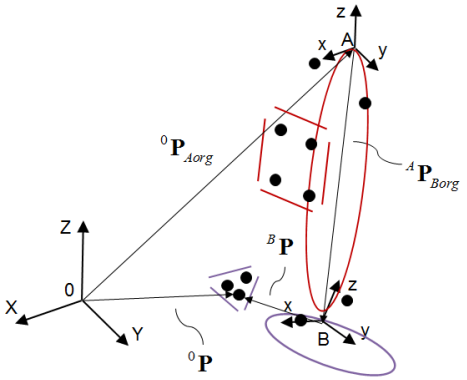

Figure 5: Representation of the local reference frame of rigid body 'B' described in the local reference frame of the rigid body 'A'.

During the static calibration the decided position is in fact used to calibrate the model in two ways: the first is to determine the transformation matrices and the respective positions of the tracking markers in the local reference frame of the body; on the other hand, after that process it is necessary to read these positions through the tracking markers. Thus, this is made through the optimization step of the kinematic consistency already shown.

When the optimum transformation matrix is obtained, if the rigid body is not a child of the global reference frame (as it happens with the exemplified rigid body B) a sequence of steps is performed in agreement with the following equations.

$$ {}^{0}\mathbf{X} = {}^{0}_{B}\mathbf{T}\,{}^{B}\mathbf{X} = {}^{0}_{A}\mathbf{T}\,{}^{A}_{B}\mathbf{T}\,{}^{B}\mathbf{X} \quad (7) $$

$$ {}^{0}_{B}\mathbf{T} = {}^{0}_{A}\mathbf{T}\,{}^{A}_{B}\mathbf{T} \Leftrightarrow {}^{A}_{B}\mathbf{T} = {}^{0}_{A}\mathbf{T}^{-1}\,{}^{0}_{B}\mathbf{T} \quad (8) $$

$$ {}^{0}_{A}\mathbf{T}^{-1} = {}^{A}_{0}\mathbf{T} = \begin{bmatrix} {}^{0}_{A}\mathbf{R}^{T} & -{}^{0}_{A}\mathbf{R}^{T}\,{}^{0}\mathbf{P}_{Aorg} \\ 0 & 1 \end{bmatrix} \quad (9) $$

Once the $^{0}_{B}\mathbf{T}$ matrix is calculated from Equation (7) it has to be decomposed on the $^{A}_{B}\mathbf{T}$ matrix, through the Equation (8). Note that a transformation matrix cannot be inverted directly but with respect to Equation (9).

The calculation of the transformation matrix of a distal rigid body in a chain (for example B in relation to A), like the $^{A}_{B}\mathbf{T}$ always involve the prior knowledge of the transformations matrices of the previous rigid bodies on the kinematic chain, therefore, there is a particular importance to obtain these matrices in the right order, starting always from the first rigid body of the chain

3.3.3. Stride Analysis during a Walking Trial

The walking trial acquisition's data files prior to be computationally analysed are manually processed in order to flag the file with the correspondent time instants of the 5 most relevant events that take place during a complete stride of a given foot: the initial contact, opposite foot's toe off, heel rise, opposite foot contact and toe off. This is done taking advantage of the AMTI's force plates in the QTM's software. One pays attention when the forces turn on and off on the plate of interest, then the event is flagged. A total of 5 trials are chosen and evaluated per each foot (a sum of 10 trials) for each one of the individuals analysed.

4. Case Study

4.1. Demographics of Control and PsA Groups

At this present moment there are not published biomechanical studies performed with a PsA population of Portuguese individuals. Both control and PsA individuals are Caucasian. The patients with PsA are selected in accordance to CASPAR[1] criteria and early disease defined as less than 2 years of disease duration. The most affected foot is registered and in cases that both feet are affected, the two are simultaneously considered as pathological. This means that among patients' feet there are 6/8 left and 4/8 right feet which are pathological. The time interval between the diagnosis date and the performance of the biomechanical assessment is 5.5 (2) months (ideally 6 months at most). Although these individuals show a higher disease duration since the first symptoms started

[1] CASPAR (ClASsification criteria for Psoriatic ARthritis) is used to confirm whether or not a patient manifests PsA. A patient must have inflammatory disease (joint, spine or entheseal) and a minimum score in specific categories (Taylor *et al*., 2006).

1.7 (0.8) years before. The demographics of the two populations are presented in Table 1.

Table 1: Demographics of the control and PsA populations in case study.

	Control Mean (SD)	PsA Mean (SD)
Number of individuals	10 (5M/5F)	8 (5M/3F)
Age (years)	29 (8)	37 (9)
Height (m)	1.71 (0.12)	1.67 (0.08)
Foot size (Eur)	39.80 (3.00)	39.75 (2.90)

4.2. Statistical Analysis with FOOTchanicsDB

The *FOOTchanicsDB* software developed in MATLAB® in the scope of this work enables users to manage their study populations and access each individual's biomechanical evaluations separately. Its main goal is to approach the clinical environment since it makes biomechanical analyses in terms of the kinematic, kinetic, plantar pressure distribution and spatiotemporal data recorded in the laboratory. It gathers all the individuals in a given database helping to perform three different comparative statistical analyses (Welch's t-test, Mann-Whitney U test and Kolmogorov-Smirnov test) between the two study populations. The previous computation methods are embedded it.

5. Results

The better way to interpret inter-segment kinematic gait patterns of individuals from the PsA population is to make a parallelism with the performed statistical study since the gait patterns for these patients in an early stage of the disease are very similar to those obtained for the healthy individuals. The inter-segment kinematic patterns obtained as mean curves of each population are represented in Figure 6 while some general statistics are presented in Table 2 along with the navicular bone height and ground reaction force's peak values. The plantar pressure distribution results are briefly presented in Table 3 and some pressure footprints of interest presented in Figure 7. Finally the spatiotemporal gait variables are shown in Table 4.

The aim of the statistical tests is to find gait parameters that differ from one population to another over the stance phase. If they are below the significance level of 5% (p<0.05) at least in one of the two Welch's t-test and Mann-Whitney U-test the result is statistically significant that does not, however, mean that is clinically relevant. Since only a few variables confirm the results as coming from two distinct distributions (*i.e.* are within the 5%) another criteria of trend analysis is presented considering *p-values* below 30% (0.05<p<0.30) (intentionally that high) which can be exploited later, in future studies covering a higher number of individuals. It must be highlight that these trend analysis' results are merely representative without any relevant clinical meaning.

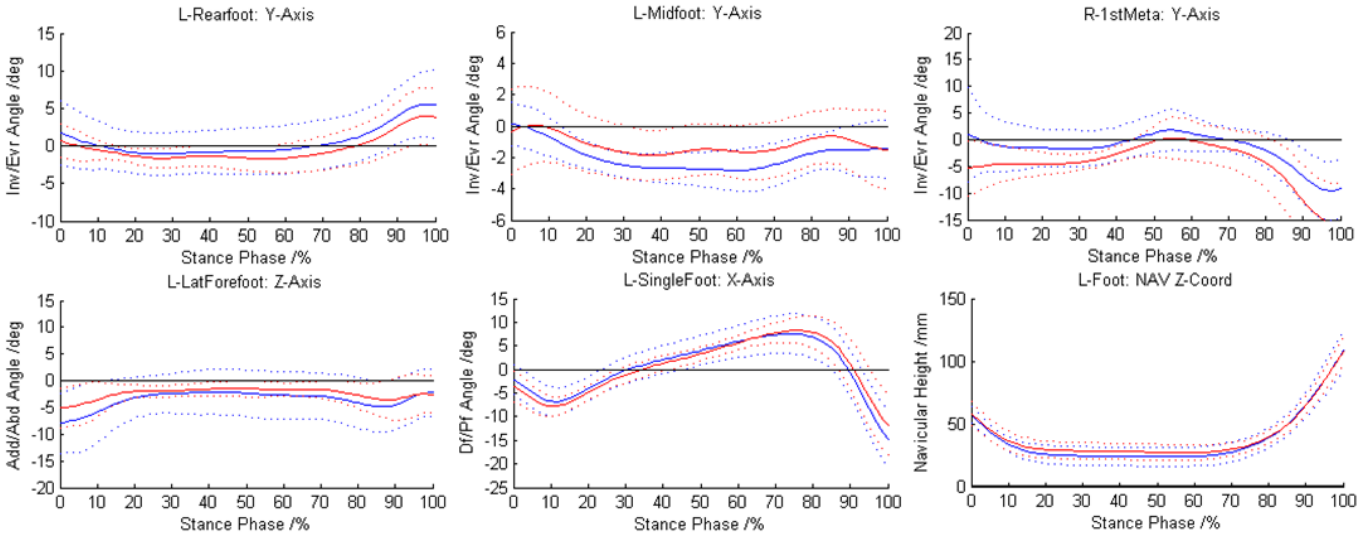

Figure 6: Inter-segment kinematics plots for each one of the rigid bodies of the biomechanical model showing the two populations mean curves (blue line represents the control population while the red line represent the PsA population. These six plots focuses mainly the most important movements within each rigid body that are relevant for distinction between the two populations: the rearfoot inversion/eversion (Inv/Evr) plot (top left); the midfoot inversion/eversion (Inv/Evr) plot (top centre); the 1st metatarsal inversion/eversion (Inv/Evr) plot (top right); the lateral forefoot adduction/abduction (Add/Abd) plot (bottom left); the single foot dorsiflexion/plantarflexion (Df/Pf) plot (bottom center); the navicular height plot (bottom right).

Table 2: Summary table covering the inter-segment kinematics and kinetics statistical results. Last column: 't' stands for trend.

Variable	Foot	Control Mean ± SE	PsA Mean ± SE	*p* (Wt)	*p* (MWU)	*p* (KS)	
Initial foot contact (deg)	**Right**	-1.60 ± 0.688	-3.74 ± 1.35	0.186	0.146	0.086	t
Terminal stance (deg)	**Left**	6.73 ± 1.41	8.68 ± 1.14	0.296	0.573	0.642	t
Peak 1stMeta dorsiflex (deg)	**Right**	6.31 ± 2.05	2.65 ± 1.11	0.140	0.203	0.243	t
Peak LFF abd (deg)	**Left**	-9.89 ± 1.91	-6.66 ± 1.48	0.200	0.173	0.376	t
1st peak GRF-AP (1 BW)	**Left**	0.165 ± 0.0117	0.149 ± 0.00541	0.241	0.173	<0.05	t
2nd peak GRF-AP (1 BW)	**Right**	0.184 ± 0.00963	0.168 ± 0.0066	0.188	0.203	0.305	t
1st peak GRF-Vert (1 BW)	**Left**	1.06 ± 0.0149	1.03 ± 0.0119	0.086	0.122	0.086	t
Lowest NAV height (mm)	**Left**	22.5 ± 2.30	26 ± 2.09	0.279	0.274	0.191	t

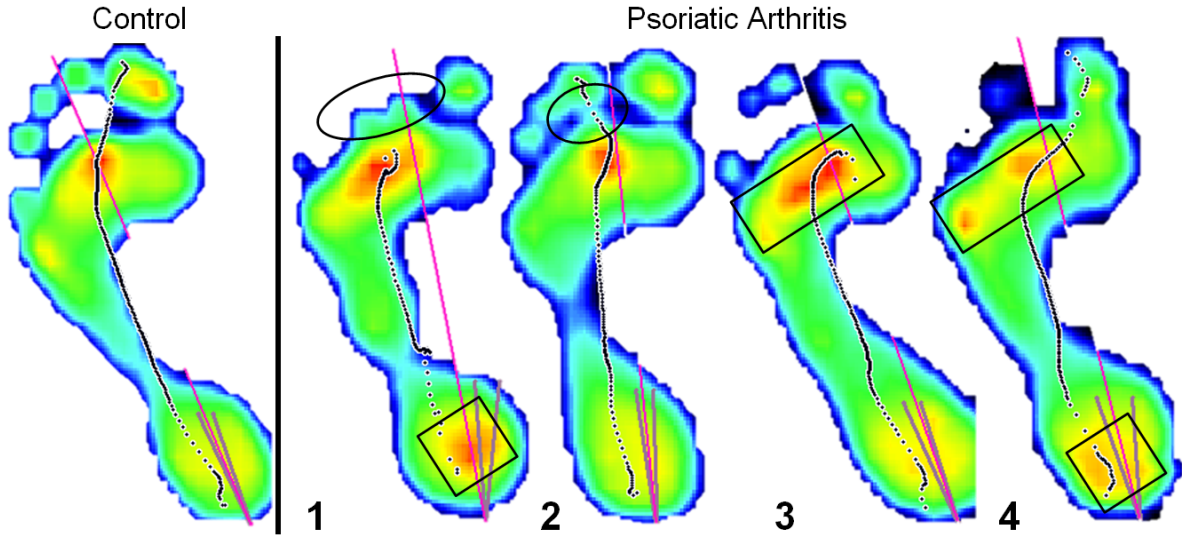

Figure 7: Comparative presentation of the plantar pressures distribution footprints between one control individual (left) and 4 different patients with PsA (1-4, right): (1) Pathological footprint presenting MTP prolongation blots (black ellipse) due to claw toes, consequent high pressures in the heads of metatarsals and high pressures in rearfoot's plantar area (under the calcaneus bone highlighted by the black square).; (2) Pathological footprint showing also the MTP prolongation blots (black ellipses) due to claw toe affecting the 2nd metatarsal head; (3) Pathological footprint endorsing the high plantar peak pressures at MTP joints that evolve later to swollen joints; (4) Pathological footprint with both MTP joint involvement and rearfoot high peak pressures, which are translated as severe mechanical loads acting on calcaneus bone. The reddish (hot) regions correspond to higher peak plantar pressures while the bluish (cold) regions correspond to lower peak plantar pressures.

Table 3: Plantar pressure distribution variables of both populations and the results of the statistical analysis. Last column: 'X' stands for statistically significant while 't' stands for trend.

Variable	Foot	Control Mean ± SE	PsA Mean ± SE	*p* (Wt)	*p* (MWU)	*p* (KS)	
Rearfoot Contact Area (%Segm)	**Right**	54.70 ± 1.55	59.80 ± 2.81	0.141	0.146	0.114	t
Rearfoot Peak pressure (kPa)	**Left**	149.00 ± 9.20	165.00 ± 13.10	0.320	0.274	0.243	t
1st meta Contact Area (%Segm)	**Right**	**64.60 ± 3.52**	**75.10 ± 1.70**	**<0.05**	**<0.05**	**0.064**	**X**
1st meta Peak pressure (kPa)	**Right**	67.40 ± 10.70	85.60 ± 12.80	0.293	0.237	0.376	t
Latffoot Contact Area (%Segm)	**Right**	**77.40 ± 1.16**	**81.00 ± 0.76**	**<0.05**	**<0.05**	**0.148**	**X**
Hallux Peak pressure (kPa)	**Left**	97.50 ± 17.20	58.40 ± 12.00	0.081	0.146	0.305	t
LesserT Contact Area (%Segm)	**Left**	50.30 ± 3.84	41.60 ± 4.51	0.165	0.146	0.243	t
LesserT Peak pressure (kPa)	**Left**	20.50 ± 4.46	11.90 ± 3.51	0.147	0.203	0.458	t

Table 4: Spatiotemporal gait variables of both populations and the results of the statistical analysis. Last column: "t" stands for trend.

Variable	Foot	Control Mean ± SE	PsA Mean ± SE	*p* (Wt)	*p* (MWU)	*p* (KS)	
Velocity		123 ± 3.97	117 ± 4.61	0.352	0.360	0.547	
Step time	**Right**	0.554 ± 0.0136	0.537 ± 0.00957	0.336	0.046	0.547	t
Step length	**Right**	67.30 ± 1.28	62.70 ± 1.83	0.060	0.055	0.191	t
Stride length	**Left**	135 ± 2.62	126 ± 3.58	0.067	0.101	0.305	t
Single support	**Right**	40.6 ± 0.52	39.7 ± 0.47	0.203	0.245	0.547	t
Double support	**Left**	19.0 ± 0.994	20.6 ± 0.835	0.243	0.515	0.642	t
Stance phase	**Left**	59.4 ± 0.505	60.4 ± 0.432	0.164	0.139	0.086	t
Swing phase	**Left**	40.6 ± 0.503	39.6 ± 0.434	0.164	0.146	0.086	t

6. Discussion

First of all, it is important to emphasize from the experience obtained from the present work that biomechanical foot models composed by a considerable number of rigid bodies, which are described through fixed anatomical axes, are error prone. Since these axes are assembled through reflective markers, the wrong maker placement on the skin will result in mistaken anatomical axes and consequently these will create offsets in gait patterns (Carson *et al*., 2001; Stebbins *et al*., 2006). The need of the anatomical axes to be orthogonal among them within the same rigid body leads the author to choose two of them, and to abdicate from the third that will result from the external product. An anatomical axis that is incorrectly defined as a rotation axis will then certainly not reproduce the correct anatomical rotation.

Furthermore, the bone landmark palpation is very difficult in all the individuals of both populations: namely the three midfoot landmarks (on the cuboid, navicular and intermediate cuneiform bones). And in addition, swollen joints along with foot pain makes almost impracticable the correct identification of the desired bone landmarks in the patients with PsA, predominantly in the midfoot and forefoot (Hyslop *et al*., 2010). Last but not least, skin based markers are vulnerable to movement artefacts even considering them as repeatable and systematic (this is confirmed by Carson *et al*. (2001)).

Even the use of the same protocol in the same individual on both lower limbs reveals that is difficult to synchronize both gait patterns obtained from each limb since even within the same individual the patterns have off-sets as well as considerable deviations. This reinforces that the correct marker placement in both legs must be taken into account and can raise some questions about performing analysis only regarding to the most affected foot in a patient with PsA, as done in Hyslop *et al*. (2010) and other studies.

Psoriatic arthritis manifests multiple inflammatory and destructive lesions in the foot such as *pes planovalgus* (flat foot), *hallux valgus* and *claw toe and d*espite the few numbers of control individuals and patients with PsA involved in this study as well as the marker placement issue, it is possible to trace some trends which majority will certainly be statistical significant with higher population (Hyslop *et al*., 2010).

Foot impairments such as *pes planovalgus* are clearly confirmed with resource to plantar pressure distribution measuring devices and also through inter-segment kinematics such as peak rearfoot eversion angle, peak midfoot inversion angle (through the "twisting" movement, although it was not reached), peak 1st metatarsal eversion angle and low ranges of motion in foot's joints (Hyslop *et al.*, 2010; Woodburn *et al*., 2004).

The peak pressures are simultaneously higher in the rearfoot and 1st metatarsal plantar areas. Although, the results are not objective in terms of the high peak pressure in the lateral forefoot as it is suggest in the literature, that together would match the calcaneus and metatarsal heads at metatarsophalangeal joints (within the 1st metatarsal and lateral forefoot). That justifies the appearance of enthesitis in those sites affecting the Achilles tendon and plantar fascia in early stages of PsA (Turner *et al*., 2008; Turner *et al*., 2006; Turner & Woodburn, 2008; Woodburn *et al*., 2004). Elevated peak pressures at metatarsophalangeal joints make the patients to off-load these painful sites by avoiding weight-transfer to the forefoot (this is the reason why the contact area in the forefoot is expected to be lower in the patients) (Turner *et al*., 2006; Turner & Woodburn, 2008; Woodburn *et al*., 2004).

Despite *claw toe* being visible with different levels of severity in some patients, no *hallux valgus* deformity was clearly evident. The subluxation of the metatarsophalangeal joint, *claw toe,* involving a metatarsal head and a proximal phalanx of a lesser toe will result in additional contact areas beyond the plantar region of the lateral forefoot which are named by the author as "metatarsophalangeal prolongation blots" or simply "MTP prolongation blots" (represented as the green regions highlighted by the black ellipses in the footprints 1 and 2 in) along with reduced contact areas in the lesser toes (Turner *et al*., 2008).

The navicular bone's height characterizes the curvature of the medial longitudinal arch of the foot which is expected to be lower for the PsA population because it characterizes the *pes planovalgus* deformation (Turner *et al*., 2008; Turner *et al*., 2006; Turner & Woodburn, 2008; Woodburn *et al*., 2004). Unfortunately, the second most erroneous results' trend stands for a higher height value in the PsA population. Obviously this minor 3 mm difference is mistaken mainly due to the difficulty of the palpation of the midtarsal bones and the consequent wrong marker placement on skin. Although this variable is very reliable on the other studies, thus there is no other explanation (Hyslop *et al*., 2010).

Adapted gait patterns are identified through the spatiotemporal variables (such as lower step time, lower step and stride lengths and higher double support time), peak ground reaction forces, peak rearfoot pressure, peak lateral forefoot pressure and terminal stance plantarflexion angle, since they mirror the

altered foot function due to pain and swollen joints. The lower 1st peak of the vertical component of the ground reaction force suggests that patients may have careful in loading the foot in the initial contact instant aiming to reduce their painful symptoms involving the calcaneus bones and adjacent biological structures such as the Achilles tendon and the plantar fascia (Turner *et al*., 2006).

This work confirms that it is possible to track biomechanical changes in patients in early stages of PsA as it was done by Turner *et al*. (2006) with patients in early stages of rheumatoid arthritis, also covering individuals whose disease duration was inferior to 2 years.

Acknowledgement

The author of this work would like to thank to his supervisor Prof. Miguel Tavares da Silva and to Elsa Vieira Sousa, MD.

References

Alonso, F. J., Cuadrado, J., Castillo, J. M. Del, & Pintado, P. (2007). Orthogonal projection methods for the kinematic data consistency of biomechanical systems. In *MULTIBODY DYNAMICS 2007 - ECCOMAS Thematic Conference* (pp. 25–28). Milano, Italy.

Carson, M. C., Harrington, M. E., Thompson, N., O'Connor, J. J., & Theologis, T. N. (2001). Kinematic analysis of a multi-segment foot model for research and clinical applications: a repeatability analysis. *Journal of Biomechanics*, *34*(10), 1299–307. Retrieved from http://www.ncbi.nlm.nih.gov/pubmed/11522309

Gottlieb, A., Korman, N. J., & Gordon, K. B. (2008). Guidelines of care for the management of psoriasis and psoriatic arthritis: section 2. Psoriatic arthritis: overview and guidelines of care for treatment with an emphasis on the biologics. *Journal of the American Academy of Dermatology*, *58*(5), 851–64.

Hyslop, E., Woodburn, J., McInnes, I. B., Semple, R., Newcombe, L., Hendry, G., … Turner, D. E. (2010). A reliability study of biomechanical foot function in psoriatic arthritis based on a novel multi-segmented foot model. *Gait & posture*, *32*(4), 619–26. doi:10.1016/j.gaitpost.2010.09.004

Jenkyn, T. R., Nichol, A., & Anas, K. (2009). Foot segment kinematics during normal walking using a multisegment model of the foot and ankle complex. *Journal of Biomechanical Engineering*, *131*(3), 034504.

Leardini, A., Benedetti, M. G., Catani, F., Simoncini, L., & Giannini, S. (1999). An anatomically based protocol for the description of foot segment kinematics during gait. *Clinical Biomechanics*, *14*(8), 528–36. Retrieved from http://www.ncbi.nlm.nih.gov/pubmed/10521637

MacWilliams, B. A., Cowley, M., & Nicholson, D. E. (2003). Foot kinematics and kinetics during adolescent gait. *Gait & Posture*, *17*, 214–24.

Nester, C., Jones, R. K., Liu, A., Howard, D., Lundberg, A., Arndt, A., Wolf, P. (2007). Foot kinematics during walking measured using bone and surface mounted markers. *Journal of Biomechanics*, *40*(15), 3412–23. doi:10.1016/j.jbiomech.2007.05.019

Ojeda, J., Mayo, J., & Martínez-Reina, J. (2011). A new method to solve kinematic consistency problem based on optimization techniques and euler parameters. In *13th World Congress in Mechanism and Machine Science* (p. IMD–123). Guanajuato, México.

Silva, M. P. T., & Ambrósio, J. A. C. (2002). Kinematic data consistency in the inverse dynamic analysis of biomechanical systems. *Multibody System Dynamics*, *8*, 219–239.

Stebbins, J., Harrington, M., Thompson, N., Zavatsky, A., & Theologis, T. (2006). Repeatability of a model for measuring multi-segment foot kinematics in children. *Gait & Posture*, *23*(4), 401–10. doi:10.1016/j.gaitpost.2005.03.002

Taylor, W., Gladman, D., Helliwell, P., Marchesoni, A., Mease, P., & Mielants, H. (2006). Classification criteria for psoriatic arthritis: development of new criteria from a large international study. *Arthritis & Rheumatism*, *54*(8), 2665–73. doi:10.1002/art.21972

Tome, J., Nawoczenski, D. A., Flemister, A., & Houck, J. (2006). Comparison of foot kinematics between subjects with posterior tibialis tendon dysfunction and healthy controls. *Journal of Orthopaedic & Sports Physical Therapy*, *36*(9), 635–44.

Turner, D E, Helliwell, P. S., Siegel, K. L., & Woodburn, J. (2008). Biomechanics of the foot in rheumatoid arthritis: identifying abnormal function and the factors associated with localised disease "impact". *Clinical Biomechanics*, *23*(1), 93–100. doi:10.1016/j.clinbiomech.2007.08.009

Turner, Deborah E, Helliwell, P. S., Emery, P., & Woodburn, J. (2006). The impact of rheumatoid arthritis on foot function in the early stages of disease: a clinical case series. *BMC musculoskeletal disorders*, *7*, 102. doi:10.1186/1471-2474-7-102

Turner, Deborah E, & Woodburn, J. (2008). Characterising the clinical and biomechanical features of severely deformed feet in rheumatoid arthritis. *Gait & Posture*, *28*(4), 574–80. doi:10.1016/j.gaitpost.2008.04.004

Van den Bogert, A. J., Smith, G. D., & Nigg, B. M. (1994). In vivo determination of the anatomical axes of the ankle joint complex: an optimization approach. *Journal of Biomechanics*, *27*(12), 1477–1488.

Winter, D. A. (1990). *Biomechanics and Motor Control of Human Movement* (2nd Ed.). Waterloo, ON, Canada: John Wiley & Sons, Inc.

Woodburn, J., Nelson, K. M., Siegel, K. L., Kepple, T. M., & Gerber, L. H. (2004). Multisegment foot motion during gait: proof of concept in rheumatoid arthritis. *Journal of Rheumatology*, *31*(10), 1918–27.